Frequency characteristic analysis of the efficiency of a MIMO array antenna with a matching circuit

Atsuhiro Kagaya [1], #Kenichi Kagoshima [2] and #Shigeki Obote[2]
[1] Graduate School of Science and Engineering, Ibaraki University
[2] The College of Engineering, Ibaraki University
4-12-1 Nakanarusawa, Hitachi, Ibaraki, 316-8511 Japan, Email:{kagosima, obote}@mx.ibaraki.ac.jp

1. Introduction

A wireless terminal antenna is required to be compact, because of the limitted space. To realize the compact array antennas for MIMO terminals, the spacing between elements should be small. This causes the strong mutual coupling between elements and mismatching at the feeding terminals. As the result, radiation efficiency deteriorates or correlation coefficient between elements increases and the performance of the MIMO system degrades.

In MIMO terminal antennas with small element spacings, it is necessary to realize the high radiation efficiency and low correlation coefficient simultaneously to achieve the high communication capacity. To overcome these problems, many researches on feeding networks for MIMO terminal antennas have been published. Wallace and Jensen successfully analyzed the feeding network using S matrix and showed that decoupling and matching could be achieved simultaneously at the designing frequency [1]. However, Lau and et.al reported that the frequency characteristic of the radiation efficiency was very narrow when the spacing of two element dipole array was around 0.1 wavelength [2]. They didn't describe which port of the array had narrow band frequency characteristics.

This paper analyzes the frequency characteristics of the radiation efficiency by employing decoupling feeding circuit and estimates the effectiveness of the decoupling and matching feeding circuit.

2. Structure of the array antenna

Fig.1(a) shows the structure of the array antenna analyzed in this paper. Two inverted L elements are located at one of the edge of the ground plate. Each element is excited through the feeding circuit which can achieve decoupling and matching for the elements. This geometry is similar to that of the antenna system shown in Fig.1(b), which consists of inverted F elements and the rectangular wire between elements instead of inverted L elements and the feeding circuit[3].

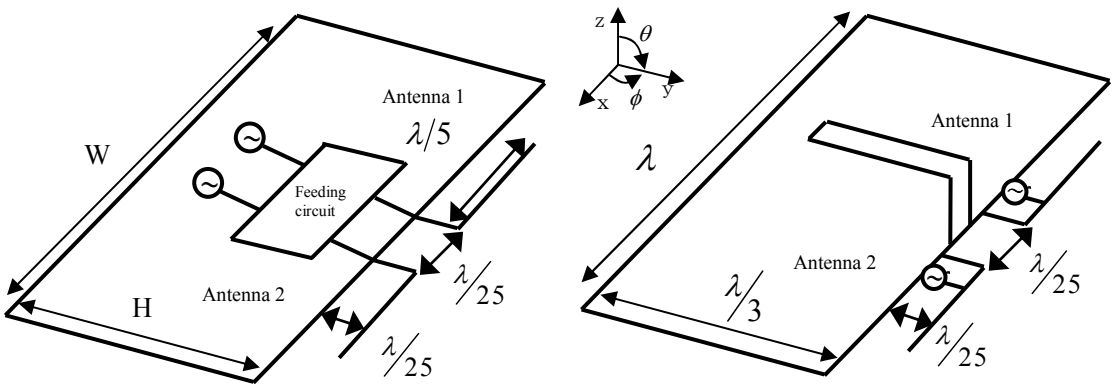

(a) Antenna of this paper (b) Antenna of reference [3]

Fig.1 Structure of array antennas

Although it is reported that the size and the shape of the rectangular wire effects to reduce the decoupling between elements, trial and error should be required to carry out its design. The design procedure of the feeding circuit shown in Fig.1(a) is described in the next section.

3. Design of matching and decoupling feeding circuit

In this section, the design procedure for a matching and decoupling feeding circuit for two element array antenna is described. Fig.2 shows the equivalent circuit of the array antenna and the feeding circuit. In Fig.2, $\bar{\bar{Y}}_a = \bar{\bar{G}}_a + j\bar{\bar{B}}_a$ is the antenna admittance matrix, $\bar{\bar{Y}}_M$ is the admittance matrix of the 2×2 matching and decoupling feeding circuit, and $\bar{\bar{Y}}_L$ is the load admittance matrix which is diagonal and Y_{Li}'s are assumed to be real. The current and voltage vector of the matching and decoupling feeding circuit are expressed as $\mathbf{I}_a = (i_1, i_2)$ and $\mathbf{V}_a = (v_1, v_2)$ at the antenna side and $\mathbf{I}_L = (I_{L3}, I_{L4}) = (i_3, i_4)$, $\mathbf{V}_L = (v_3, v_4)$ at the load side. An input current vector of the antenna is $\mathbf{I'}_a = -\mathbf{I}_a = (I_{a1}, I_{a2})$ and a source current vector is $\mathbf{I}_0 = (I_{03}, I_{04})$. When the sub matrix of $\bar{\bar{Y}}_M$ is expressed by $\bar{\bar{Y}}_{ij}$ (i=1,2, j=1,2), the following fundamental equations are derived.

$$\mathbf{I}_a = \bar{\bar{Y}}_{11}\cdot\mathbf{V}_a + \bar{\bar{Y}}_{12}\cdot\mathbf{V}_L \quad (1) \qquad \mathbf{I}_L = \bar{\bar{Y}}_{21}\cdot\mathbf{V}_a + \bar{\bar{Y}}_{22}\cdot\mathbf{V}_L \quad (2)$$

$$\mathbf{I'}_a = -\mathbf{I}_a = \bar{\bar{Y}}_a\cdot\mathbf{V}_a \quad (3) \qquad \mathbf{I}_L = \mathbf{I}_0 - \bar{\bar{Y}}_L\cdot\mathbf{V}_L \quad (4)$$

The condition for matching between the antenna and the feeding circuit is that the input admittance towards the circuit from the plane 1-1' and 2-2' is equal to the complex conjugate transpose of the antenna admittance $\bar{\bar{Y}}_a$. Considering this condition and that $\bar{\bar{Y}}_M$ is lossless, the following equations, which determine the sub matrixes of $\bar{\bar{Y}}_M$, are derived, when the diagonal elements of $\bar{\bar{Y}}_L$ are all assumed to be equal to Y_0.

$$\bar{\bar{B}}_{11} = -\bar{\bar{B}}_a \quad (5) \qquad \bar{\bar{B}}_{22} = 0 \quad (6) \qquad \bar{\bar{B}}_{12}\bar{\bar{B}}_{21} = Y_0\bar{\bar{G}}_a \quad (7)$$

Using matrix elements of $\bar{\bar{B}}_{12} = \bar{\bar{B}}_{21}^T$, eq.(7) is decomposed and expressed by the following equations.

$$b_{13}^2 + b_{14}^2 = Y_0 g_{a11} \quad (8) \qquad b_{13}b_{23} + b_{14}b_{24} = Y_0 g_{a12} \quad (9) \qquad b_{23}^2 + b_{24}^2 = Y_0 g_{a22} \quad (10)$$

To solve the equations from (8) to (10), b_{ij}'s are expressed using trigonometric functions, which satisfy the equations (8) and (10), as follows.

$$b_{13} = \sqrt{Y_0 g_{a11}}\cos\alpha \quad (11) \qquad b_{14} = \sqrt{Y_0 g_{a11}}\sin\alpha \quad (12) \qquad b_{23} = \sqrt{Y_0 g_{a22}}\cos\beta \quad (13) \qquad b_{24} = \sqrt{Y_0 g_{a22}}\sin\beta \quad (14)$$

Substituting eq.(11)~(14) into eq.(9), the relation between α and β has been found and the following equation is obtained.

$$\beta = \alpha - \cos^{-1}\left(g_{a12}/\sqrt{g_{a11}\cdot g_{a22}}\right) \quad (15)$$

Consequently, all circuit elements can be determined using antenna admittance $g_{ij} + jb_{ij}$(i=1,2, j=1,2) and arbitrary parameter α.

On the other hand, the admittance matrix $\bar{\bar{Y}}_{fa}$ towards the circuit from the plane 3-3' and 4-4', when the antenna is connected to the feeding circuit, is derived from ep.(1)~(4) as follows,

$$\bar{\bar{Y}}_{fa} = \bar{\bar{Y}}_{22} - \bar{\bar{Y}}_{21}\bar{\bar{Y}}_a^{-1}\left\{I + \bar{\bar{Y}}_{11}\bar{\bar{Y}}_a^{-1}\right\}^{-1}\bar{\bar{Y}}_{12} \quad (16)$$

The admittance matrix $\bar{\bar{Y}}_{fa}$ can be transformed into the scattering matrix $\bar{\bar{S}}$ by the next equation, where the normalized admittances at the input and output ports are Y_0.

$$\bar{\bar{S}} = \begin{pmatrix} S_{33} & S_{34} \\ S_{43} & S_{44} \end{pmatrix} = \left(I + \bar{\bar{Y}}'_{fa}\right)^{-1}\left(I - \bar{\bar{Y}}'_{fa}\right) \quad (17)$$

Then efficiency evaluated at each feeding port can be expressed as follows, using the elements of the scattering matrix given by (17).

$$\eta_3 = 1 - |S_{33}|^2 - |S_{43}|^2 \quad (18) \qquad \eta_4 = 1 - |S_{44}|^2 - |S_{34}|^2 \quad (19)$$

4. Results of the analysis

Fig.3 shows the frequency characteristics of the efficiency at each feeding port. The size of the ground plane are $W = \lambda$ and $H = \lambda/3$. The frequency characteristic of the #3 port and the #4 port are different each other. When the one port is wideband, the other port is narrowband. Fig.4 shows bandwidths of Fig.3. The bandwidths are estimated at $\eta = 0.75, 0.80$ and 0.90, respectively. When α is 15[deg.], the bandwidth of 27% is attained at #4 port, which is the widest at $\eta = 0.75$. On the other hand, at #3 port, it is about 3% which is the narrowest. When α is 62[deg.], both bandwidths of #3 port and #4 port are almost equal and are 5%. Although the increase at #3 port is small, the degradation from 27% to 5% at #4 port is significant.

Fig.5 shows the frequency characteristics of the efficiency when the width of the ground plane W is changed. Here, α is chosen to be 0[deg.]. The efficiency of #4 port is affected by W, although the one of #3 port hardly depends on W. Fig.6 shows the bandwidths of $\eta = 0.75$ at #3 and #4 port, respectively. When W is about one wavelength, the bandwidth becomes maximum and is about 23%.

Fig.7 shows the frequency characteristics of the efficiency when the height of the ground plane H is changed. α is also chosen to be 0[deg.]. The efficiency of #4 port is affected by H, although the one of #3 port hardly depends on W. Fig.8 shows the bandwidths of $\eta = 0.75$ at #3 and #4 port, respectively. When H is about 0.1λ, the bandwidth becomes maximum and is about 32%. When α is chosen to be 62 [deg.], the bandwidth of both ports are equal and is about 5%. This result is the same when the ground plate is $W = \lambda$ and $H = \lambda/3$.

5. Conclusion

This paper discussed the frequency characteristic of the radiation efficiency of an array antenna with a matching and decoupling feeding circuit. Frequency characteristic is different at each of feeding port. The widest bandwidth is about 27%, and the narrowest bandwidth is about 3% at $\eta = 0.75$. When the bandwidths are adjusted to be equal at both feeding ports by parameter α, the ones of 5% are attained. Total bandwidth with η greater than 0.75 is 10% which is smaller than the former. The dependence of the bandwidth on the ground plane size has been also investigated. The bandwidth of the one port is affected significantly and the one of the other port hardly changed. Maximum bandwidth of 32% has been obtained when the width W is λ and the height H is 0.1λ.

References

[1] J. W. Wallace and M. A. Jensen, “Mutual coupling in MIMO wireless system : A rigorous network theory analysis”, IEEE Trans. on Wireless Com. vol.3 , No.4, pp1317-1325, July 2004.

[2] B. K. Lau, J. B. Andersen, G. Kristensson, A. F. Molisch, “Impact of Matching Network on Bandwidth of Compact Antenna Array”, IEEE Trans. on AP, vol.54, no.11, pp3225-3238, Nov. 2006.

[3] T. Ohishi, N. Oodachi, S. Obayashi, H. Shoki, T. Morooka, “Optimization of Folded Parasitic Element for Reduction of Mutual Coupling between antennas”, Proc. of 2008 IEICE General Conference, B-1-200, Mar. 2008.

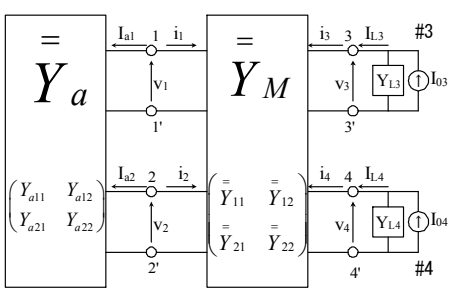

Fig.2 Equivalent circuit of the array antenna and the feeding circuit

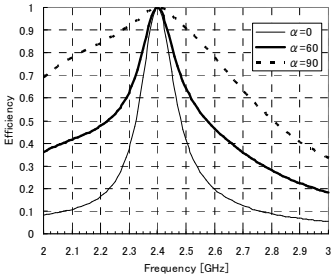

(a) #3 port

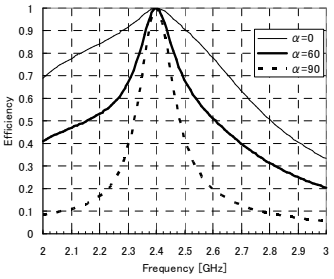

(b) #4 port

Fig.3 Frequency characteristic of efficiency

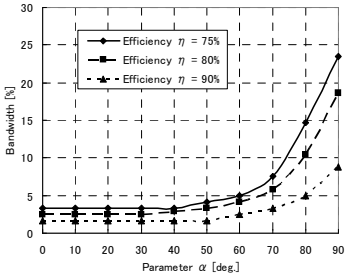

(a) #3 port

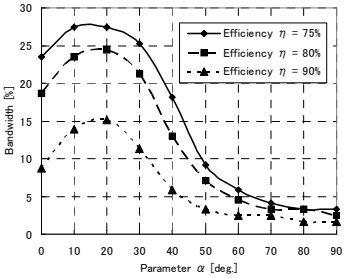

(b) #4 port

Fig.4 Bandwidth of each port versus parameter α

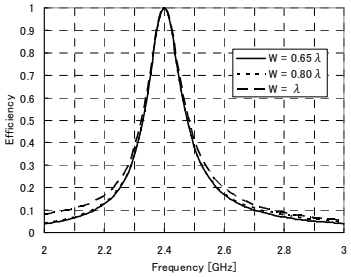

(a) #3 port

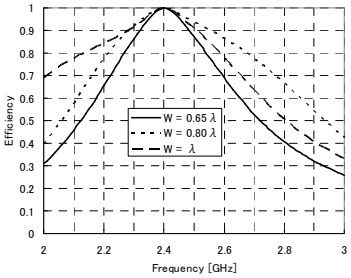

(b) #4 port

Fig.5 Frequency characteristic of efficiency versus ground plane width W (α = 0 [deg.])

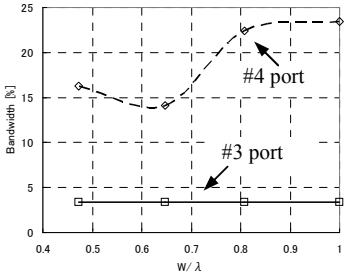

Fig.6 Bandwidth of 75% in Fig.5 (α = 0 [deg.])

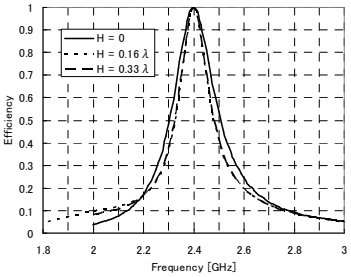

(a) #3 port

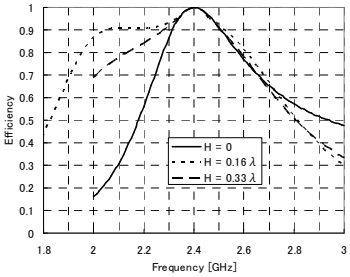

(b) #4 port

Fig.7 Frequency characteristic of efficiency versus ground plane height H (α = 0 [deg.])

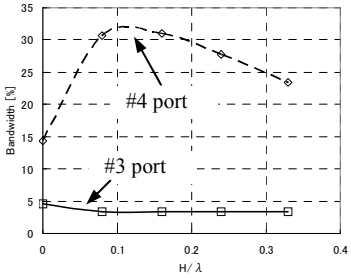

Fig.8 Bandwidth of 75% in Fig.7 (α = 0 [deg.])